



Article

Photon-shielding properties of alkali- and acid-treated Philippine natural zeolite

Mon Bryan Z. Gili 

Philippine Nuclear Research Institute, Department of Science and Technology, Diliman, Quezon City, Philippines and Materials Science and Engineering Program, College of Science, University of the Philippines Diliman, Quezon City, Philippines

Abstract

The effects of chemical treatment on the radiation-shielding properties of Philippine natural zeolites were investigated using *EpiXS* following the EPICS2017 library. The zeolites were studied using X-ray diffraction and energy-dispersive X-ray spectroscopy. The acid treatment eliminated Fe and Ca, having a negative impact on the cross-section of the HCl-modified zeolite. The mass attenuation coefficients of the raw, NaOH- and HCl-modified zeolites at 1332 keV were 0.0545, 0.0544 and 0.0548 cm² g⁻¹, respectively. At 100–10,000 keV, the linear attenuation coefficient depends on the density and increases in the order HCl-modified > NaOH-modified > raw zeolite. In the energy range of 100–16,000 keV, the mean free path and half-value layer values are in the order of HCl-modified < NaOH-modified < raw zeolite. The raw and NaOH-modified zeolites have comparable effective atomic numbers, whereas the HCl-treated zeolite has significantly lower such values.

Keywords: EPICS2017, *EpiXS*, gamma-rays, natural zeolite, photon attenuation

(Received 3 May 2023; revised 17 August 2023; Accepted Manuscript online: 11 September 2023; Editor: George Christidis)

Natural materials such as clays, rocks, ores and soils have long been studied regarding their photon-shielding applications as they have unique properties that are useful for attenuating ionizing radiation, in addition to being low cost and in great abundance. The gamma-shielding capabilities of ball clay and kaolin from south-western Nigeria were investigated experimentally and theoretically by Olukotun *et al.* (2018). The radiation attenuation factors of red clay, ball clay, bentonite and kaolin were determined experimentally by Elsafi *et al.* (2021), and the shielding parameters of halloysite were computed theoretically by Mansour *et al.* (2020). Several minerals were also used as aggregates to enhance the radiation-shielding properties of concrete, including colemanite (Oto *et al.*, 2019), barite and hematite (Masoud *et al.*, 2020), magnetite (Jozwiak-Niedzwiedzka *et al.*, 2018) and sepiolite (Sayyed *et al.*, 2018). Previous work has reported the potential use of various ores such as barite, magnetite, limonite, hematite and serpentine ores (Oto *et al.*, 2015), amethyst ore (Korkut *et al.*, 2011) and various types of boron ores (Demir, 2010; Korkut *et al.*, 2012) as shielding materials. Soils have also received considerable attention in radiation-shielding studies. Pires (2022) reported the attenuation capabilities of highly weathered soils from Brazil. In addition, Akman *et al.* (2019) and Sayyed *et al.* (2019) assessed the shielding characteristics of various soils from Turkey, and Hila *et al.* (2021b) computed theoretically the photon-shielding parameters of mangrove forest soils across the Philippines using various computer software programs. Lunar soil has also been evaluated as a shielding material against radiation in space (Miller *et al.*, 2009).

One fascinating material that has shown potential in shielding applications is zeolite. Zeolites are microporous crystalline aluminosilicate minerals built of [SiO₄] and [AlO₄]⁻ tetrahedra (Ratel *et al.*, 2022). They have a structure characterized by a framework of linked tetrahedra, each consisting of four oxygen atoms surrounding a silicon or aluminium cation (Wise, 2013). This three-dimensional network has open cavities in the form of channels and cages, which are occupied by H₂O molecules and extra-framework cations. Most of the common natural zeolites are formed by alteration that occurs in volcanic rocks when in contact with fresh water or sea water. In the Philippines, natural zeolites occur in the Albay and Pangasinan provinces. The Philippines' natural zeolite production quantities in 2010, 2011, 2012 and 2013 were 244, 435, 478 and 550 tons, respectively (Philippine Statistics Authority (Mines and Geosciences Bureau), 2013). These zeolites are suitable candidates for radiation-shielding composites because they have comparable mass attenuation coefficients (μ_m) to clays and soils and slightly smaller μ_m than that of concrete (Gili & Hila, 2021a). In addition, numerous studies have reported the use of natural zeolites in radiation-shielding applications.

The chemical composition and radiation attenuation properties of a clinoptilolite-rich natural zeolite from Turkey were investigated by Kurudirek Murat *et al.* (2010). These authors reported that trace radioactive elements were present in the zeolite and that this zeolite has a poorer attenuation efficiency in the ionizing X-ray region of the electromagnetic spectrum than Portland cement (PC). Akkurt *et al.* (2010) studied the radiation shielding of concrete containing various concentrations of zeolite aggregates and reported that the linear attenuation coefficient (μ) decreased with increasing concentration of zeolite aggregates. However, the neutron-shielding properties of bricks manufactured

Email: mbzgili@pnri.dost.gov.ph

Cite this article: Gili MBZ (2023). Photon-shielding properties of alkali- and acid-treated Philippine natural zeolite. *Clay Minerals* 58, 258–266. <https://doi.org/10.1180/clm.2023.25>

from a brick clay obtained from Bartın, Turkey, increased by as much as three-fold upon the addition of 20% zeolite compared to the bricks without additional zeolite (Cay *et al.*, 2014). Further increasing in the zeolite content by up to 30% decreased the macroscopic neutron cross-section substantially, which was smaller than that of the bricks free of zeolite. The radiation attenuation coefficients of PC mixed with natural zeolite were examined by Türkmen *et al.* (2008). In the energy range of 4–10 keV, the addition of natural zeolite decreased radiation attenuation. However, at a lower energy level (1.5–4.0 keV), the addition of zeolite tended to increase radiation attenuation.

Certain techniques can be employed to enhance the shielding properties of zeolites, such as to incorporating heavy elements like lead (Pb; Puišo *et al.*, 2013). Pb-doped zeolites were added to cement, and this blended cement demonstrated improved X-ray-shielding properties (Palubinskas *et al.*, 2022). The shielding characteristics of zeolites can be modified *via* chemical treatment. No studies have yet been conducted regarding this matter, and the current study aims to address this research gap. This work explores the possibility of modifying the photon-shielding properties of Philippine natural zeolite through alkali and acid treatment using NaOH and HCl solutions, respectively. *EpiXS* software is used to determine the photon-shielding properties of raw and chemically modified zeolites through the EPICS2017 library. These properties include the photon cross section (σ), linear attenuation coefficient (LAC), mass attenuation coefficient (MAC), half-value layer (HVL), tenth-value layer (TVL), mean free path (MFP), effective atomic number (Z_{eff}) and effective electron density (N_{eff}) in the X-ray and gamma-ray energy ranges of 1–10⁶ keV. The shielding parameters are compared to those of PC.

Materials and methods

Sample preparation

The natural zeolite used was supplied by LITHOS Manufacturing, OPC, Philippines. It was mined from Mangatarem Town, Pangasinan, in northern Luzon, Philippines. The chemical composition of the raw zeolite, as presented in a previous study (Gili *et al.*, 2020), is shown in Table 1. The major components of natural zeolite are SiO₂ and Al₂O₃, comprising 55.29% and 12.63%, respectively. Significant amounts of CaO and Fe₂O₃ are also present (4.69% and 3.43%, respectively). The zeolite shows 7.04% weight loss at 105°C and 14.71 wt.% loss on ignition (LOI), which is attributed to its tightly bound water content.

The natural zeolite was pre-treated with acidic and basic solutions. Firstly, a 1.5 M NaOH solution was prepared by dissolving

NaOH pellets (Merck, 99%) in deionized (DI) water. This concentration was selected because it was the optimum concentration for modifying the zeolite for adsorption applications (Ates & Akgül, 2016). Then, 25 g of zeolite was added to 250 mL of the NaOH solution and soaked for 6 h. The suspension was filtered and washed with 1 L of DI water, and the solid was dried for 5 h at 150°C. Then, the zeolite was soaked in 250 mL of 4 M NaCl solution (Mallinckrodt, analytical reagents). This step was necessary to maintain the homoionic quality of the zeolite. Then, the sample was rinsed with 0.5 L of DI water three times. In the final washing step, drops of 1 M HCl solution were added to bring the pH to neutral. The powder was then collected, dried for 5 h at 150°C and ground with an agate pestle and mortar for 20 min.

Similarly, a 3.8 M HCl solution was prepared (Merck, fuming 37%) in DI water. Then, 25 g of zeolite was added to 250 mL of HCl solution, soaked for 6 h, washed with 1 L of DI water and dried for 5 h at 150°C. Subsequently, the sample was soaked in 250 mL of 4 M NaCl solution for 24 h and rinsed with 0.5 L DI water three times. In the final washing step, drops of 1 M NaOH solution were added to bring the pH to neutral. The zeolite powder was dried for 5 h at 150°C and ground.

To measure the density of zeolite in solid/pellet form, ~0.25 g of each zeolite sample was placed on a 13 mm-diameter stainless steel die (Graseby-Spec) and pelletized using a uniaxial press (SPEX 3630 X-PRESS) with a pressure of 2–3 tons. The holding and release durations were both 2 min.

Characterization

The structure and crystal order of the raw, NaOH-modified and HCl-modified zeolites were analysed using X-ray diffraction (XRD; Shimadzu, XRD-7000 Maxima) with Cu-K α (1.5406 Å) radiation at 40 kV and 30 mA. A continuous scan was performed at a scanning speed of 2° min⁻¹ with a step size of 0.02°. The chemical composition of the samples was determined by scanning electron microscopy (SEM; SU1510, Hitachi High Technologies) coupled with energy-dispersive X-ray spectroscopy (EDS; Thermo Scientific Noran System 7) at an accelerating voltage of 15 kV.

Shielding parameter calculation

The X-ray- and gamma-shielding characteristics of the raw and chemically modified Philippine natural zeolites were determined using a *Windows*-based interpolation software called *EpiXS* (Hila *et al.*, 2021a). The software is based on the Monte Carlo transport library known as Electron Photon Interaction Cross Section 2017 (EPICS2017; Cullen, 2018) of the Evaluated Nuclear Data File version B-VIII (ENDF/B-VIII; Brown *et al.*, 2018). It is user-friendly and can be downloaded from the Philippine Nuclear Research Institute's website at <https://www.pnri.dost.gov.ph/index.php/downloads/software>. The photon cross-section (σ), MAC, LAC, HVL, TVL, MFP, Z_{eff} and N_{eff} are among the photon-shielding parameters considered.

The chemical composition and the density of the materials are input into the software's interface to compute the abovementioned parameters. For reference, the radiation-shielding parameters of PC were also obtained. The chemical composition of PC is listed in Table 2 (Bilal *et al.*, 2019). It has a specific gravity of 3.05, which translates to a density of 3.05 g cm⁻³. The LOI is attributed to the moisture content (H₂O).

Table 1. Chemical components of the Philippine natural zeolite.

Component	Amount (%)
SiO ₂	55.29
Al ₂ O ₃	12.63
Fe ₂ O ₃ ^a	3.43
MgO	1.49
CaO	4.69
Na ₂ O	0.62
K ₂ O	0.58
H ₂ O ^b	7.04
LOI ^c	14.71

^aAssumed as cubic γ -Fe₂O₃.

^bLoss at 105°C.

^cLOI (H₂O).

Table 2. Chemical composition of PC.

Component	CaO	SiO ₂	Al ₂ O ₃	MgO	SO ₃	Fe ₂ O ₃	Na ₂ O	K ₂ O	LOI
Wt.%	63.47	22.00	5.50	1.70	1.82	3.50	0.20	1.00	0.64

Theoretical aspects

The parameter σ (barns atom⁻¹) is a useful concept for characterizing the attenuation of radiation in materials. It represents the likelihood that photons will interact with matter in a certain process. In a compound or mixture, σ may be thought of as a weighted average of the cross-sections of the individual component elements as given in Equation 1, where f_i is the i th element's atom fraction (Gili & Hila, 2021b):

$$\sigma = \sum f_i \sigma_i \quad (1)$$

The total atomic cross-section (σ_T) is the sum of the component cross-sections (Equation 2), where σ_{PE} , σ_{coh} , σ_{incoh} , σ_{PP-N} , σ_{PP-E} are the photoelectric cross-section, coherent scattering cross-section, incoherent scattering cross-section, pair production in the nuclear field cross-section and pair creation in the electron field (or triplet production) cross-section, respectively (Gili & Hila, 2021a).

$$\sigma_T = \sigma_{PE} + \sigma_{coh} + \sigma_{incoh} + \sigma_{PP-N} + \sigma_{PP-E} \quad (2)$$

The cross-section and the MAC or μ_m (cm² g⁻¹) are connected (Equation 3), where A_i is the atomic mass of the i th element and N_A is Avogadro's number (Gili & Jeong, 2023). The MAC is the likelihood of an interaction between incoming photons and matter in a given unit area per unit mass.

$$\mu_m = \sigma \frac{N_A}{\sum f_i A_i} \quad (3)$$

The MAC is connected to the shielding material's density (g cm⁻³) through the LAC, or μ (cm⁻¹; Equation 4; Plando *et al.*, 2023):

$$\mu_m = \frac{\mu}{\rho} \quad (4)$$

where ρ is the bulk density of the material. The LAC is the likelihood of photon interaction in one of the ways mentioned above per unit length. It can be calculated experimentally using the Beer–Lambert relation between the incident photon intensity, I_0 (Equation 5), and the ratio of the transmitted intensity, I , across the shielding material's thickness, x (Gili & Hila, 2021b):

$$\mu = \frac{\ln\left(\frac{I_0}{I}\right)}{x} \quad (5)$$

The HVL (cm) is the thickness of the material through which an input photon loses 50% of its original intensity, and it is calculated from Equation 6 (Gili & Hila, 2021b). It is obtained from the Beer–Lambert relation. The shielding improves with decreasing HVL.

$$x = \frac{\ln(2)}{\mu} = \frac{0.693}{\mu} \quad (6)$$

The MFP (cm) is the average distance a photon may travel inside a material before interacting with it. The MFP is related to the LAC (Equation 7; Gili & Hila, 2021b):

$$\text{MFP} = \frac{1}{\mu} \quad (7)$$

The σ_T can be calculated from Equation 8 (Hussein *et al.*, 2022):

$$\sigma_T = \frac{1}{N_A} \sum_i f_i A_i (\mu_m)_i \quad (8)$$

Equation 9 is used to determine the total electronic cross-section, σ_e (barns atom⁻¹), or the likelihood that photons will interact with electrons. In Equation 9, Z_j is the atomic number of the j th element (Limkitjaroenporn *et al.*, 2011; Hussein *et al.*, 2022):

$$\sigma_e = \frac{1}{N_A} \sum_j f_j \frac{A_j}{Z_j} (\mu_m)_j \quad (9)$$

An essential factor that describes the shielding material's characteristics in terms of photon absorption and scatter interactions is Z_{eff} . Z_{eff} refers to the overall electronic and atomic cross-section (Equation 10; Limkitjaroenporn *et al.*, 2011; Yasaka *et al.*, 2014):

$$Z_{\text{eff}} = \frac{\sigma_T}{\sigma_e} \quad (10)$$

Equation 11 is used to calculate N_{eff} , or the number of electrons in the shielding material per unit mass, where A is the mean atomic mass, equal to $\sum_i f_i A_i$ (Yasaka *et al.*, 2014; Hussein *et al.*, 2022):

$$N_{\text{eff}} = \frac{N_A}{A} Z_{\text{eff}} = \frac{N_A}{\sum_i f_i A_i} Z_{\text{eff}} = \frac{\mu_m}{\sigma_e} \quad (11)$$

Results and discussion

Characterization

Structure and crystal order. The X-ray traces of the raw and chemically modified natural zeolites are presented in Fig. 1. Most peaks that were indexed are attributed to clinoptilolite- and mordenite-type zeolites, which are the main components of this natural zeolite. The broad peak at $\sim 5.5^\circ 2\theta$ ($d_{(001)} \approx 16 \text{ \AA}$) corresponds to montmorillonite. Traces of quartz were also present in the material. Upon treatment with NaOH solution, the intensity of the montmorillonite peak was significantly reduced and broadened, indicating partial dissolution. The decrease in intensities of all of the peaks relative to that of raw zeolite indicates an inferior crystal order, perhaps due to the desilication of the zeolites (i.e. the removal of Si atoms in the zeolite framework; Wang *et al.*, 2016). However, acid treatment resulted in the total disappearance of the montmorillonite peak, suggesting the destruction of the crystal structure. The intensities of all of the indexed peaks were significantly reduced, which implies poorer crystal order, possibly due to dealumination (i.e. the leaching of Al; Beyer, 2002).

Chemical composition. The chemical compositions of the zeolites determined by EDS are summarized in Table 3. The raw

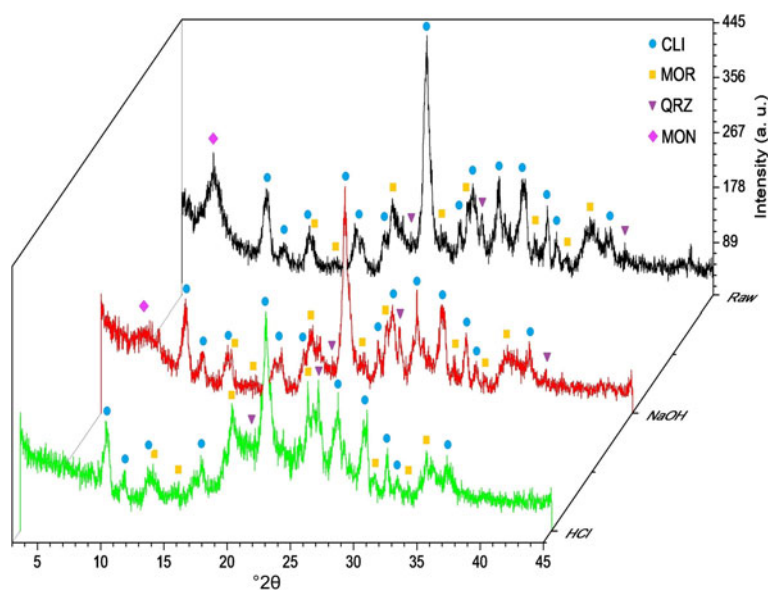


Figure 1. XRD traces of the (a) raw, (b) NaOH-modified and (c) HCl-modified zeolites. CLI = clinoptilolite; MON = montmorillonite; MOR = mordenite; QRZ = quartz.

Table 3. Chemical compositions of the raw and chemically modified zeolites determined by EDS.

Component	Raw zeolite (wt.%)	NaOH-modified zeolite (wt.%)	HCl-modified zeolite (wt.%)
SiO ₂	58.2	55.6	75.7
Al ₂ O ₃	12.7	11.9	12.1
Fe ₂ O ₃	14.5	14.1	–
MgO	2.9	3.7	2.2
CaO	4.5	3.0	–
Na ₂ O	–	4.2	3.8
CO ₂	7.1	7.5	6.2
Pellet density (g cm ⁻³)	1.12	1.36	1.45

zeolite is primarily composed of SiO₂ and Al₂O₃ owing to the aluminosilicate structure of the zeolite. A significant amount of Fe₂O₃ is also present in the material, which is in agreement with our previous studies (Gili *et al.*, 2019, 2020). Minor CaO, MgO and Na₂O are also present. Alkali treatment slightly lowered the amount of SiO₂, probably due to the dissolution of the silicate minerals. However, acid treatment resulted in the leaching of Fe and Ca. The chemical composition was entered into *EpiXS* to calculate the various radiation-shielding parameters of the samples. The measured pressed bulk densities of the raw, NaOH- and HCl-modified zeolites were 1.12, 1.36 and 1.45 g cm⁻³, respectively. The chemically treated zeolites, especially the HCl-modified ones, have greater pressed bulk densities, despite them having lower Ca and Fe concentrations. This suggests that a partially destroyed zeolite framework due to dealumination or desilication is easier to compress upon pelletization.

Radiation shielding properties

Atomic cross-section. Figure 2a shows the total photon cross-section (σ_T) of the raw and chemically modified natural zeolites as well as the reference material, PC. Except for PC, the alkali-treated zeolite has the highest σ_T among the three samples

because it has the highest Fe content. The raw zeolite has a comparable σ_T with the NaOH-modified zeolite, as they have almost the same Fe content. Iron has the greatest cross-section among the elements as it has the highest atomic number (Fig. 2b). Therefore, Fe and Ca are the elements that most affect the value of σ_T . By contrast, the acid-treated zeolite had the lowest σ_T as it essentially is free of Fe and Ca. In general, X-ray and gamma-ray interactions are most likely to occur according to the order of PC > NaOH-modified zeolite > raw zeolite > HCl-modified zeolite.

Mass attenuation coefficient. The MACs of the raw and chemically modified natural zeolites and the reference material, PC, are shown in Fig. 3. The MAC follows a similar trend to σ_T as the former is proportional to the latter. The MAC has high values for low X-ray energies (<10² keV) but decreases as the photon energy increases. Hence, low-energy photons such as X-rays are more likely to be attenuated than high-energy photons such as gamma-rays. Notably, the MACs of all of the samples at energies of 10²–10⁴ keV are comparable. However, above 10⁴ keV, PC had the highest MAC value, whereas the HCl-modified zeolite had the lowest MAC value. The MACs of the raw and NaOH-treated zeolites are comparable in this energy range.

The MAC values at selected gamma-ray energies are shown in Table 4. At a low gamma-energy of 60 keV, there are significant differences among the MAC values. Except for PC, the NaOH-modified zeolite had the highest MAC, followed by the raw zeolite, with the HCl-treated zeolite having the lowest MAC. At 356–1332 keV, the MAC values are comparable except for PC, which has a greater MAC than the zeolite samples in the entire energy range considered.

Linear attenuation coefficient. The computed LACs of the raw and chemically modified zeolites and PC are illustrated in Fig. 4. The LAC indicates how efficiently a material absorbs the energy of an incident photon per unit length. There is a clear trend regarding the order in which one material attenuates photons better than the others. At 10–100 keV, the LAC was as follows: PC > NaOH-modified zeolite > raw zeolite > HCl-modified zeolite. At 10²–10⁴ keV, the order is PC > HCl-modified zeolite > NaOH-modified zeolite > raw zeolite. And at >10⁴ keV, the

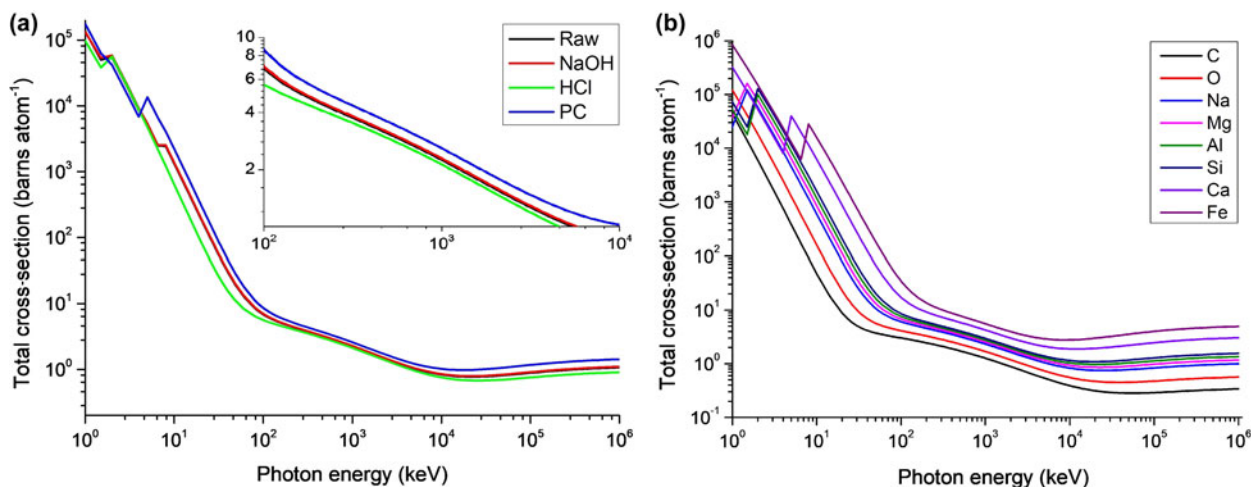


Figure 2. Total photon cross-section of (a) the zeolite samples and PC and (b) the elemental components of the raw zeolite.

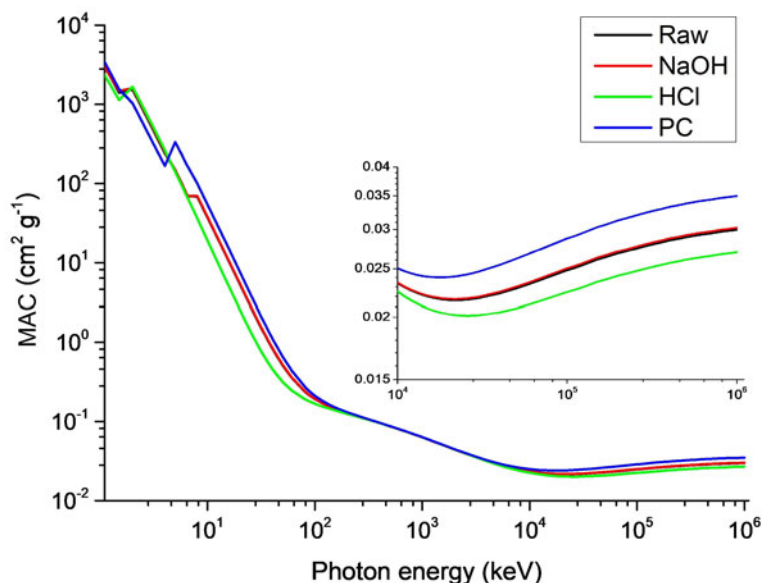


Figure 3. MACs of the zeolite samples and PC.

Table 4. Computed MACs ($\text{cm}^2 \text{g}^{-1}$) of the zeolite samples and PC using *EpiXS*.

Radioisotope	Energy (keV)	Raw	NaOH	HCl	PC
Am-241	60	0.3702	0.3740	0.2532	0.4576
Ba-133	356	0.1001	0.0999	0.1000	0.1015
Cs-137	662	0.0766	0.0764	0.0769	0.0773
Co-60	1173	0.0582	0.0580	0.0584	0.0587
Co-60	1332	0.0545	0.0544	0.0548	0.0550

order is PC > NaOH-modified zeolite > HCl-modified zeolite > raw zeolite. Note that the LAC is just the MAC multiplied by the density of the material. For comparable MAC values at energies of 10^2 – 10^4 keV, the order of density values (PC > HCl-modified zeolite > NaOH-modified zeolite > raw zeolite) will dictate the ranking of LAC in this energy range. In quantifying the photon-attenuation capability of a material, MAC is more appropriate than LAC, as the latter changes with the density. The compaction of the material will enhance the LAC due to the

increase in density. However, as mentioned above, LAC can be calculated experimentally through the Beer–Lambert relation.

Mean free path and half-value layer. The effectiveness of a material at shielding radiation may be visualized through the MFP and HVL. The MFP is the average distance a photon can travel within a material without being interrupted (or interacted with). Thus, lower MFP values indicate that the material can attenuate photons better, as only a thin layer of the material will induce photon interaction (or interruption). Materials with lower MFPs are generally favoured because they can attenuate ionizing radiation better than those with greater MFPs. **Figure 5a** shows the MFPs of the zeolite samples together with PC. At 100–16,000 keV, the order is PC < HCl-modified zeolite < NaOH-modified zeolite < raw zeolite. Hence, after PC, HCl-treated zeolite is the best shielding material. However, at >16,000 keV, the order of MFP values is PC < NaOH-modified zeolite < HCl-modified zeolite < raw zeolite, which means that NaOH-modified zeolite is the best shielding material among the zeolite samples in this energy range.

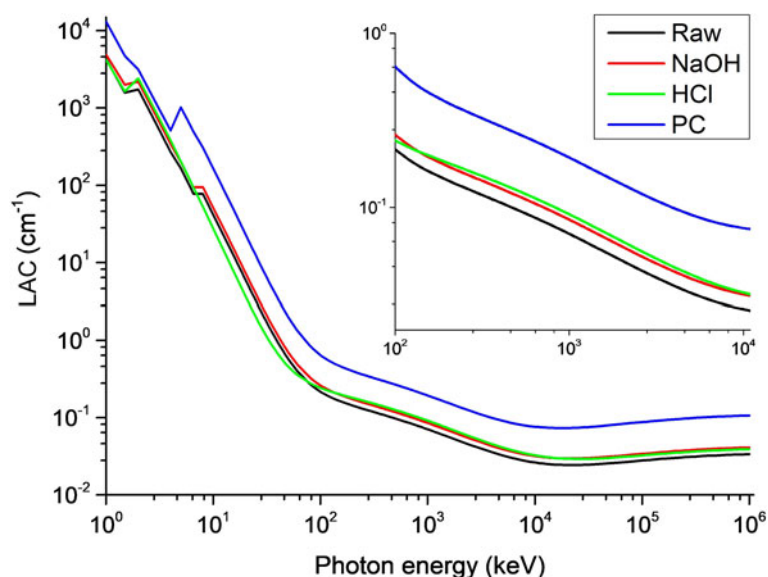


Figure 4. LACs of the zeolite samples and PC.

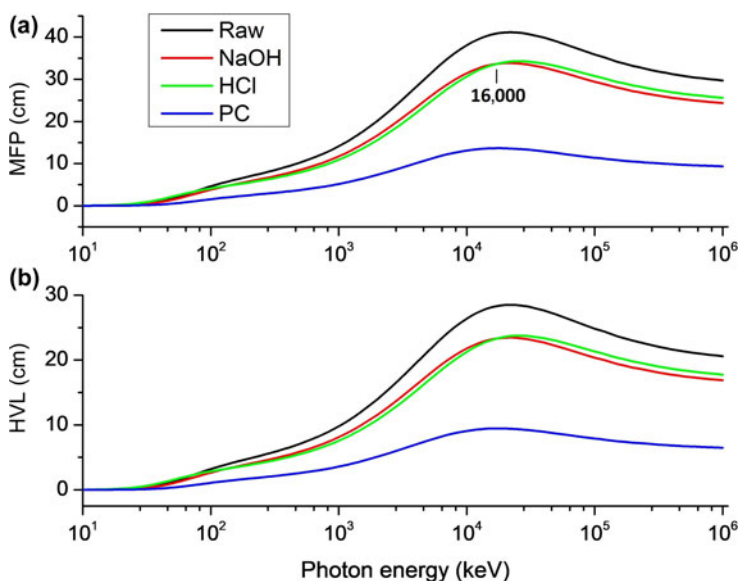


Figure 5. Plots of (a) MFP and (b) HVL of the zeolite samples and PC.

To further simplify the concept of radiation shielding, HVL is sometimes preferred. HVL refers to the thickness of a material in which the intensity of a photon is reduced by half upon passing through it. The HVL is just the MFP multiplied by a constant, $\ln(2)$ or 0.693. Thus, the plot of the HVL vs photon energy (Fig. 5b) is identical to that of MFP vs photon energy (Fig. 5a). Similarly, materials with lower MFPs are considered better shielding. Table 5 lists the HVLs of the samples at selected gamma-radiation energies. The acid-treated zeolite had the lowest HVL values among the zeolite samples at all of the energies considered, which is largely because it has the greatest density. It is worth mentioning that MFP and HVL are also influenced by density, similarly to LAC. Hence, MFP and HVL may improve upon compaction of the material.

LAC, MFP and HVL are all dependent on the bulk density of the material. At a microscopic level, the zeolite structure would affect the shielding properties of zeolite, as the zeolite framework

Table 5. Computed HVLs (cm) of the zeolite samples and PC using *EpiXS*.

Radioisotope	Energy (keV)	Raw	NaOH	HCl	PC
Am-241	60	1.6657	1.3648	1.8905	0.4967
Ba-133	356	6.1597	5.1076	4.7883	2.2401
Cs-137	662	8.0500	6.6767	6.2258	2.9384
Co-60	1173	10.6031	8.7947	8.1900	3.8739
Co-60	1332	11.3171	9.3869	8.7417	4.1344

is related to the presence of channels/cavities, which are associated with the porosity and, hence, the density of the material. The alkali and acid treatments increase the porosity and thus decrease the apparent density of the material. Thus, the LACs, MFPs and HVLs of these chemically treated zeolites, especially the HCl-modified zeolite, should be inferior to the raw zeolite. This might be true if the zeolites were not pelletized. As

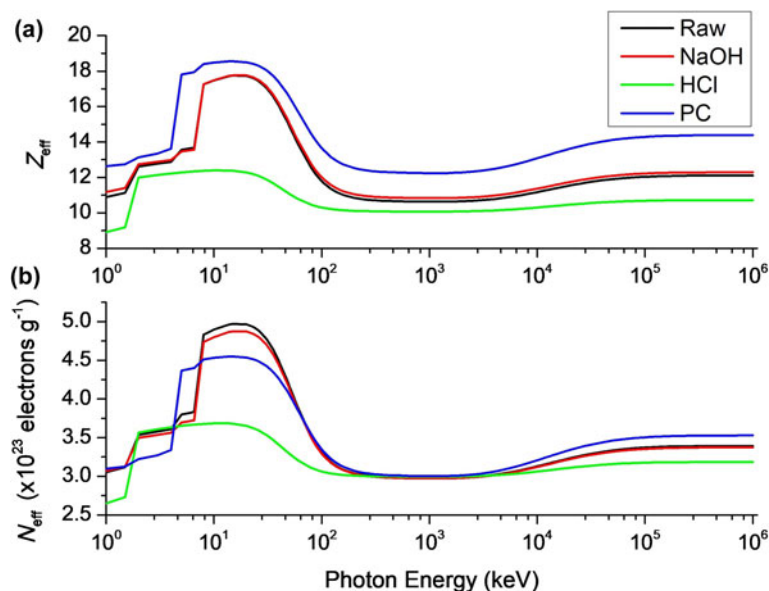


Figure 6. Plots of (a) Z_{eff} and (b) N_{eff} of the zeolite samples and PC.

desilication and dealumination result in a weaker structural framework, they are easily compressed upon pelletization. A more compacted material has a larger pressed bulk density, thereby increasing LAC, MFP and HVL.

Effective atomic number and effective electron density. The atomic number Z refers to the number of protons in an element. The number of protons dictates how many electrons surround the nucleus, which in most cases determines the chemical behaviour of an element. For molecules and mixtures, the total interaction can be represented by a parameter called the effective atomic number (Z_{eff} ; Toker *et al.*, 2021). This parameter is important for predicting how photons such as X-rays interact with a substance, as certain types of interactions depend on the atomic number. The Z_{eff} reflects the radiation attenuation capability of the material, as shielding parameters depend directly on the atomic number.

The Z_{eff} values are the greatest for PC across the entire energy range of 1– 10^6 keV (Fig. 6a). Raw and NaOH-modified zeolites have comparable Z_{eff} values, whereas HCl-treated zeolite has a significantly lower Z_{eff} value, which can be attributed to the lack of Fe and Ca.

The Z_{eff} energy reflects the relative importance of partial photon interaction processes. For the raw and alkali-treated zeolites, photoelectric absorption at X-ray energies ($E < 65$ keV), incoherent (Compton) scattering at low to intermediate gamma-ray energies ($65 < E < 16,000$ keV) and pair production in the nuclear field at high gamma-ray energies ($E > 16,000$ keV) are the dominant photon interaction processes. Coherent (Rayleigh) scattering is not important in this context because it occurs primarily at low energies, where photoelectric absorption is by far the most important interaction process. Pair production in the electron field occurs at high gamma-ray energies but is dominated by pair production in the nuclear field. The highest Z_{eff} value is 17.74, which occurs at 15 keV. This value represents the material's mean atomic number (Manohara *et al.*, 2008). However, the lowest value is ~ 10.60 , occurring at 300–2500 keV.

The Z_{eff} is related to the N_{eff} , which exhibits similar behaviour (Fig. 6b). Because incident photons interact with individual electrons, a higher N_{eff} means greater photon attenuation (Sahadath *et al.*, 2015). In the energy range $8 < E < 60$ keV, where

photoelectric absorption is dominant, the N_{eff} values of the raw and NaOH-modified zeolites are greater than those of PC and HCl-treated zeolite. At the intermediate energy range of 300–2500 keV, the N_{eff} values are comparable for all of the zeolite samples, as well as the reference material. At $>10^4$ keV, the values are ranked in the order of PC > raw zeolite > NaOH-modified zeolite > HCl-modified zeolite.

Conclusions

The effects of chemical modification on the photon attenuation capabilities of Philippine natural zeolite were investigated using the EPICS2017 photoatomic library interpolated using the *EpiXS* software. The change in the chemical composition upon acid and alkali treatment affected the shielding parameters significantly. The leaching of Fe and Ca upon treatment with HCl reduced the photon cross-section of the zeolite, which in turn decreased the values of other shielding parameters such as the MAC, Z_{eff} and N_{eff} . Thus, potential chemical reactions leading to the removal of the certain elements from zeolites should be avoided when they are employed as a shielding material or used to fabricate radiation-shielding composites (e.g. zeolite-blended concrete). However, NaOH modification did not provide substantial improvements regarding the shielding parameters of the natural zeolite. Nevertheless, the radiation attenuation efficiency of a material can be improved, as certain parameters, such as LAC, MFP and HVL, which all depend on the density of the material, can be enhanced upon compaction of the material.

Acknowledgements. The author is grateful to the Earth Materials Science Laboratory of the National Institute of Geological Sciences, University of the Philippines Diliman, for the XRD analysis and the GAEA Research Laboratory of the University of the Philippines Manila for the SEM-EDX analysis. Special thanks are also given to LITHOS Manufacturing, OPC, which supplied the zeolite used in this study.

Financial support. The author did not receive support from any organization for the submitted work.

Conflicts of interest. The author certifies that he has no affiliations with or involvement in any organization or entity with any financial interest or non-

financial interest in the subject matter or materials discussed in this manuscript.

Data availability. The datasets generated and/or analysed during the current study are available from the author upon reasonable request.

References

- Akkurt I., Akyildirim H., Mavi B., Kilincarslan S. & Basyigit C. (2010) Radiation shielding of concrete containing zeolite. *Radiation Measurements*, **45**, 827–830.
- Akman F., Turan V., Sayyed M.I., Akdemir F., Kaçal M.R., Durak R. & Zaid M.H.M. (2019) Comprehensive study on evaluation of shielding parameters of selected soils by gamma and X-rays transmission in the range 13.94–88.04 keV using WinXCom and FFAST programs. *Results in Physics*, **15**, 102751.
- Ates A. & Akgül G. (2016). Modification of natural zeolite with NaOH for removal of manganese in drinking water. *Powder Technology*, **287**, 285–291.
- Beyer H.K. (2002) Dealumination techniques for zeolites. Pp. 203–255 in: *Post-Synthesis Modification I* (H.G. Karge & J. Weitkamp, editors). Springer, Berlin, Germany.
- Bilal H., Yaqub M., Ur Rehman S.K., Abid M., Alyousef R., Alabduljabbar H. & Aslam F. (2019) Performance of foundry sand concrete under ambient and elevated temperatures. *Materials*, **12**, 2645.
- Brown D.A., Chadwick M.B., Capote R., Kahler A.C., Trkov A., Herman M.W. *et al.* (2018) ENDF/B-VIII.0: the 8th major release of the Nuclear Reaction Data Library with CIELO-project cross sections, new standards and thermal scattering data. *Nuclear Data Sheets*, **148**, 1–142.
- Cay V.V., Sutcu M., Gencel O. & Korkut T. (2014) Neutron radiation tests about FeCr slag and natural zeolite loaded brick samples. *Science and Technology of Nuclear Installations*, **2014**, 971490.
- Cullen D. (2018) *A Survey of Photon Cross Section Data for Use in EPICS2017*, IAEA-NDS-225, rev. 1. International Atomic Energy Agency, Vienna, Austria, 61 pp.
- Demir F. (2010) Determination of mass attenuation coefficients of some boron ores at 59.54 keV by using scintillation detector. *Applied Radiation and Isotopes*, **68**, 175–179.
- Elsafi M., Koraim Y., Almurayshid M., Almasoud F.I., Sayyed M.I. & Saleh I.H. (2021) Investigation of photon radiation attenuation capability of different clay materials. *Materials*, **14**, 6702.
- Gili M.B.Z. & Hila F.C. (2021a) Characterization and Radiation shielding properties of Philippine natural bentonite and zeolite. *Philippine Journal of Science*, **150**, 1475–1488.
- Gili M.B.Z. & Hila F.C. (2021b) Investigation of gamma-ray shielding features of several clay materials using the EPICS2017 library. *Philippine Journal of Science*, **150**, 1017–1026.
- Gili M.B.Z. & Jecong J.F.M. (2023) Radiation shielding properties of ZnO and other glass modifier oxides: BaO, MgO, Na₂O, and TiO₂, using EpiXS software. *Arabian Journal for Science and Engineering*, **48**, 1021–1029.
- Gili M.B.Z., Olegario-Sanchez L. & Conato M. (2019) Adsorption uptake of Philippine natural zeolite for Zn²⁺ ions in aqueous solution. *Journal of Physics: Conference Series*, **1191**, 012042.
- Gili M.B.Z., Pares F.A., Nery A.L.G., Guillermo N.R.D., Marquez E.J. & Olegario E.M. (2020) Changes in the structure, crystallinity, morphology and adsorption property of gamma-irradiated Philippine natural zeolites. *Materials Research Express*, **6**, 125552.
- Hila F.C., Asuncion-Astronomo A., Dingle C.A.M., Jecong J.F.M., Javier-Hila A.M.V., Gili M.B.Z. *et al.* (2021a) EpiXS: a Windows-based program for photon attenuation, dosimetry and shielding based on EPICS2017 (ENDF/B-VIII) and EPDL97 (ENDF/B-VI.8). *Radiation Physics and Chemistry*, **182**, 109331.
- Hila F.C., Dicen G.P., Javier-Hila A.M.V., Asuncion-Astronomo A., Guillermo N.R.D., Rallos R.V. *et al.* (2021b) Determination of photon shielding parameters for soils in mangrove forests. *Philippine Journal of Science*, **150**, 245–256.
- Hussein K.I., Alqahtani M.S., Alzahrani K.J., Alqahtani F.F., Zahran H.Y., Alshehri A.M. *et al.* (2022) The effect of ZnO, MgO, TiO₂, and Na₂O modifiers on the physical, optical, and radiation shielding properties of a TeTaNb glass system. *Materials*, **15**, 1844.
- Jozwiak-Niedzwiedzka D., Glinicki M.A., Gibas K. & Baran T. (2018) Alkali-silica reactivity of high density aggregates for radiation shielding concrete. *Materials*, **11**, 2284.
- Korkut T., Korkut H., Karabulut A., & Budak G. (2011) A new radiation shielding material: amethyst ore. *Annals of Nuclear Energy*, **38**, 56–59.
- Korkut T., Karabulut A., Budak G., Aygün B., Gencel O. & Hançerlioğullari A. (2012) Investigation of neutron shielding properties depending on number of boron atoms for colemanite, ulexite and tincal ores by experiments and FLUKA Monte Carlo simulations. *Applied Radiation and Isotopes*, **70**, 341–345.
- Kurudirek Murat M., Özdemir Y., Türkmen I. & Levet A. (2010) A study of chemical composition and radiation attenuation properties in clinoptilolite-rich natural zeolite from Turkey. *Radiation Physics and Chemistry*, **79**, 1120–1126.
- Limkitjaroenporn P., Kaewkhao J., Limsuwan P. & Chewpraditkul W. (2011) Physical, optical, structural and gamma-ray shielding properties of lead sodium borate glasses. *Journal of Physics and Chemistry of Solids*, **72**, 245–251.
- Manohara S.R., Hanagodimath S.M., Thind K.S. & Gerward L. (2008) On the effective atomic number and electron density: a comprehensive set of formulas for all types of materials and energies above 1 keV. *Nuclear Instruments and Methods in Physics Research Section B: Beam Interactions with Materials and Atoms*, **266**, 3906–3912.
- Mansour A., Sayyed M.I., Mahmoud K.A., Şakar E. & Kovaleva E.G. (2020) Modified halloysite minerals for radiation shielding purposes. *Journal of Radiation Research and Applied Sciences*, **13**, 94–101.
- Masoud M.A., Kansouh W.A., Shahien M.G., Sakr K., Rashad A.M. & Zayed A.M. (2020) An experimental investigation on the effects of barite/hematite on the radiation shielding properties of serpentine concretes. *Progress in Nuclear Energy*, **120**, 103220.
- Miller J., Taylor L., Zeitlin C., Heilbronn L., Guetersloh S., DiGiuseppe M. *et al.* (2009) Lunar soil as shielding against space radiation. *Radiation Measurements*, **44**, 163–167.
- Olukotun S.F., Gbenu S.T., Ibitoye F.I., Oladejo O.F., Shittu H.O., Fasasi M.K. & Balogun F.A. (2018) Investigation of gamma radiation shielding capability of two clay materials. *Nuclear Engineering and Technology*, **50**, 957–962.
- Oto B., Yildiz N., Akdemir F. & Kavaz E. (2015) Investigation of gamma radiation shielding properties of various ores. *Progress in Nuclear Energy*, **85**, 391–403.
- Oto B., Madak Z., Kavaz E. & Yaltay N. (2019) Nuclear radiation shielding and mechanical properties of colemanite mineral doped concretes. *Radiation Effects and Defects in Solids*, **174**, 899–914.
- Palubinskas P., Puišo J., Vaičiukynienė D., Kielė A., Baltušnikas A. & Vaitkevičius V. (2022) X-ray radiation shielding properties of zeolite blended cements. Pp. 444–447 in: *Radiation Interaction with Materials: Fundamentals and Applications: 5th International Conference "Radiation Interaction with Materials: Fundamentals and Applications 2014": Program and Materials* (A. Grigonis, editor). Technologija, Kaunas, Lithuania.
- Philippine Statistics Authority (Mines and Geosciences Bureau) (2013) *Mines and Minerals Philippine Yearbook 2013*. Philippine Statistics Authority, Quezon City, Philippines, 25 pp.
- Pires L.F. (2022). Radiation shielding properties of weathered soils: influence of the chemical composition and granulometric fractions. *Nuclear Engineering and Technology*, **54**, 3470–3477.
- Plando F.R.P., Gili M.B.Z. & Maquiling J.T. (2023) Microstructural characterizations and radiation shielding quantities of rice husk ash-based self-compacting concrete and its precursors. *Radiation Physics and Chemistry*, **208**, 110916.
- Puišo J., Jakevičius L., Vaičiukynienė D., Vaitkevičius V., Kantautas A. & Baltušnikas A. (2013) X-ray shielding zeolite containing lead. *Medical Physics in the Baltic States*, **1**, 119–123.
- Ratel L., Kuznik F. & Johannes K. (2022) Open sorption systems. Pp. 526–541 in: *Encyclopedia of Energy Storage*, vol. 1 (L.F. Cabeza, editor). Elsevier, Amsterdam, The Netherlands.
- Sahadath H., Mollah A.S., Kabir K.A. & Fazlul Huq M. (2015) Calculation of the different shielding properties of locally developed ilmenite-magnetite (I–M) concrete. *Radioprotection*, **50**, 203–207.

- Sayyed M.I., Tekin H.O., Kılıcoglu O., Agar O. & Zaid M.H.M. (2018) Shielding features of concrete types containing sepiolite mineral: comprehensive study on experimental, XCOM and MCNPX results. *Results in Physics*, **11**, 40–45.
- Sayyed M.I., Akman F., Turan V. & Araz A. (2019) Evaluation of radiation absorption capacity of some soil samples. *Radiochimica Acta*, **107**, 83–93.
- Toker O., Bilmez B., Akçalı Ö., Özşahin Toker M. & İçelli O. (2021) Practical simulation method for determination of effective atomic number from Rayleigh to Compton scattering ratio by MCNP. *Radiation Physics and Chemistry*, **181**, 109330.
- Türkmen I., Özdemir Y., Kurudirek M., Demir F., Simsek Ö. & Demirboğa R. (2008) Calculation of radiation attenuation coefficients in Portland cements mixed with silica fume, blast furnace slag and natural zeolite. *Annals of Nuclear Energy*, **35**, 1937–1943.
- Wang Y., Yokoi T., Namba S. & Tatsumi T. (2016) Effects of dealumination and desilication of beta zeolite on catalytic performance in *n*-hexane cracking. *Catalysts*, **6**, 8.
- Wise W.S. (2013) MINERALS | Zeolites. *Reference Module in Earth Systems and Environmental Sciences*. Retrieved from <https://doi.org/10.1016/B978-0-12-409548-9.02906-7>
- Yasaka P., Pattanaboonmee N., Kim H.J., Limkitjaroenporn P. & Kaewkhao J. (2014) Gamma radiation shielding and optical properties measurements of zinc bismuth borate glasses. *Annals of Nuclear Energy*, **68**, 4–9.